Confirmation of the Modified Bean Model from Simulations of Superconducting Vortices

R. A. Richardson, O. Pla,* and F. Nori†
Physics Department, The University of Michigan, Ann Arbor, Michigan 48105-1120
(Received 15 July 1993)

From a very simple description of vortices and pinning centers, we obtain nonlinear density profiles of vortices in type-II dirty superconductors that result from changing an external magnetic field. The results confirm a modified Bean model description of these systems, following the Kim empirical form that relates the current inside the material to the local magnetic field. We also obtain realistic magnetization hysteresis loops and examine the discrete evolution of the density profiles in our systems. This evolution is not continuous, but takes place by the occurrence of avalanches of vortices promoted by the addition or extraction of vortices from the edges of the system.

PACS numbers: 74.60.Ge, 05.60.+w

Over the past three decades, the Bean model [1] for the magnetization of hard type-II superconductors in a varying external magnetic field has been successfully applied to a variety of experimental phenomena. In most applications, the Bean form for the flux density profiles within a sample can only be inferred from bulk quantities such as the magnetization, and details about the internal field are hard to come by. One means of providing specific information about the behavior of flux lines within a material is through computer simulation (see, e.g., [2,3]). In this work, we simulate the development of Bean-type profiles in a one dimensional system with a random array of pinning centers. We examine the dependence of these profiles on various parameters and demonstrate that the only physical elements necessary to achieve Bean-like behavior are repulsive forces between vortices and attractive forces between vortices and pinning centers. We also investigate the evolution of these profiles and find that the dynamics of vortices within these systems obey power laws suggestive of self-organized criticality [4]. The literature on vortices and the Bean model is vast and we do not attempt a review. The interested reader is directed to Refs. [5,6] and the papers cited therein for a more complete discussion.

Our samples are one dimensional, with periodic boundary conditions (i.e., the sample is a ring). Pinning centers of uniform depth are distributed randomly over most of the sample, with a small region left pin-free from which vortices are either added or extracted. This pin-free region, as will be explained more fully below, can be thought of as the region where the "external field" is applied.

For the interaction between vortices and pinning centers we will consider the latter to be represented by parabolic potentials. These potentials have a finite range, which is given by the constant ξ_p. Explicitly, the total pinning potential acting on vortex i is

$$V_{pi}=\sum_j\left(-\frac{f_c\xi_p}{2}+\frac{f_c}{2\xi_p}(x_i^v-x_j^p)^2\right)\Theta(\xi_p-|x_i^v-x_j^p|), \quad (1)$$

where x_i^v and x_j^p represent the position of the ith vortex and the jth pinning site, respectively. $\Theta(x)$ is the Heaviside step function and f_c is the force needed to detach one vortex from one pinning center in the one body problem, or, in other words, the strength of the pinning well.

The interaction between vortices is much better understood than that between vortices and material defects (pinning sites). Several theoretical methods (see, for instance, Ref. [5]) lead to a vortex-vortex potential which varies as a modified Bessel function. The evaluation of this potential for a system with many vortices is very costly in terms of simulation time, and we therefore approximate it by the following simple parabolic form:

$$V_{vi}=\sum_{j,j\neq i}A_v(|x_i^v-x_j^v|-\xi_v)^2\Theta(\xi_v-|x_i^v-x_j^v|), \quad (2)$$

where A_v is the strength of the potential and ξ_v is the vortex-vortex interaction range. This range, like that for the vortex-pinning interaction, is taken to be finite. We neglect the hard core part in the potential, where the material is normal. This corresponds to assuming that the Ginzburg-Landau parameter κ is large.

The simulation consists of two procedures which correspond to slowly ramping up and ramping down the external field. Vortices are either added or extracted and the system is then allowed to relax to equilibrium. If friction is neglected, the total force that acts on vortex i in the presence of other vortices and pinning centers is $\boldsymbol{\mathcal{F}}_i=-\boldsymbol{\nabla}_i V_{pi}-\boldsymbol{\nabla}_i V_{vi}$. We exploit the fact that $\boldsymbol{\mathcal{F}}_i$ is linear in x_i^v in 1D to calculate successive configurations of the flux lattice. This is performed iteratively by updating x_i^v in such a way that $\boldsymbol{\mathcal{F}}_i$ vanishes, where we take as input the x_j^v calculated in the previous step. Throughout this work, the dimensions of length and force will be referenced to ξ_v and f_c; i.e., $\xi_v=1$ and $f_c=1$. The free parameters are thus A_v, N_p, and ξ_p.

The simulations are performed by randomly distributing N_p pinning centers over 80% of the system. A 20% chunk is left unpinned. The pinned region corresponds to the actual sample. Within the pinning region, the pins

0031-9007/94/72(8)/1268(4)$06.00

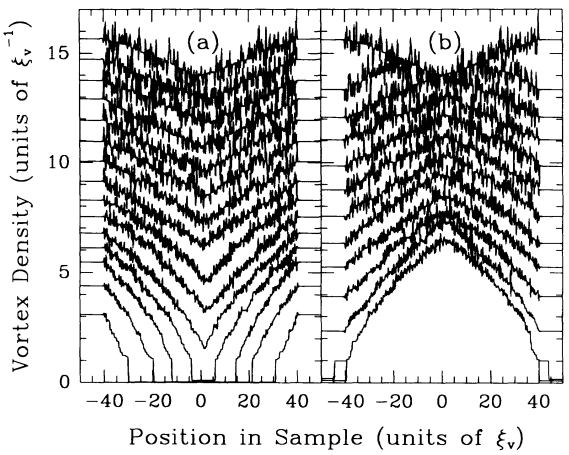

FIG. 1. Vortex density profiles for the (a) ramp-up phase and (b) ramp-down phase for a simulation with a pin density of 30 per unit length and $A_v = 5$. The flat plateaus on either side of the sample show the density in the unpinned region and the jagged V-shaped profiles correspond to the density in the pinned region.

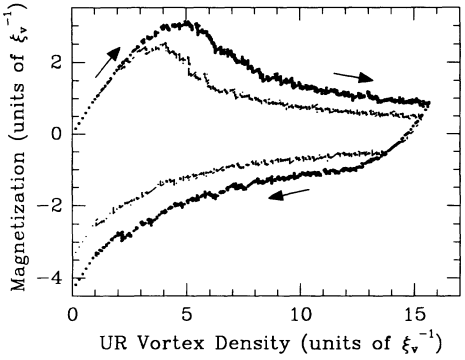

FIG. 2. Magnetization curves for two simulations. The outer, darker curve is for a pin density of 30 and the inner curve is for a pin density of 15. Both samples have $A_v = 5$. The x axis is the vortex density in the unpinned region (UR), which corresponds to external field.

are distributed quite densely (with an average density from 10 to 30 per unit length) but the pinning range ξ_p is made small enough that the probability of pins overlapping is quite low ($\xi_p = 0.005$ for all data presented here). This is done to avoid complicated pinning landscapes where some local pinning regions are much deeper than others due to pin overlap. In general, then, the pinning force in our models is provided by narrow, weak, and densely distributed pins of uniform depth.

In the "ramp-up" phase of the simulation, vortices are successively added to the unpinned region and in the "ramp-down" phase, they are extracted from this region. First, let us consider the ramp-up phase. The first few vortices added to the system remain in the unpinned region (UR) until, after a time, enough vortices have been added that they cannot all remain in the unpinned region without overlapping. At this point, vortices begin to be forced into the pinned region (PR) of the sample. This process is impeded by the pinning forces encountered when a vortex enters the PR. As more vortices are added, other vortices are gradually pushed farther into the PR, in both directions, until the two developing "flux fronts" meet in the middle of the PR. This situation corresponds to reaching the full penetration field H^* discussed in Bean's work [1]. We then continue to add vortices (up to 1600) until the system is quite densely packed. The results of one such simulation are shown in Fig. 1(a). In this figure, the circular sample is cut in the middle of the UR and unfolded for visualization purposes. The plot is of vortex density (which is proportional to field) versus distance across the sample. One can clearly see the development of Bean-like flux profiles, where the flux density is highest on the edges of the sample and lowest in the middle. The density in the UR can be thought of as the "external" field and the design of the simulation is such that the boundary condition of the internal field at the edges of the sample being equal to the external field is automatically met.

Starting from the configuration that results upon the completion of the ramp-up phase, we then successively remove vortices from the UR and allow the system to relax as before. This procedure is continued until all vortices are removed from the UR. The configuration at this point corresponds to the remnant magnetization peak which results when an external field is raised to some value and then brought back down to zero. The results of a ramp-down simulation are shown in Fig. 1(b). Again, Bean-like behavior is evident, including the characteristic "gull-wing" shaped profiles which result when the memory of the initial configuration before the ramp-down is not yet erased.

Exploiting the analogy between density in the UR and external field, the results can be used to calculate a magnetization hysteresis loop for the sample. In actuality, we create a partial loop since our simulation does not readily allow for a reversal of field direction. The density in the UR is taken to be the external field and the integrated difference between this field and the internal field across the sample yields the magnetization. This result is illustrated in Fig. 2 for two different pin densities.

An interesting feature of the profiles shown in Fig. 1 is that one can observe a clear trend in the slope of the flux density as a function of field. This slope corresponds to the critical current J_c in real samples, and it can be seen to decrease as the local field increases. This variation in J_c leads to curved profiles, rather than the linear profiles in the classical Bean picture. Such a variation is often described as "modified" Bean behavior and several forms of modification have been previously proposed.

One of the earliest of these was put forward in Ref. [7] shortly after Bean's original work. There, the authors define a maximum pinning force α_m and find empirically

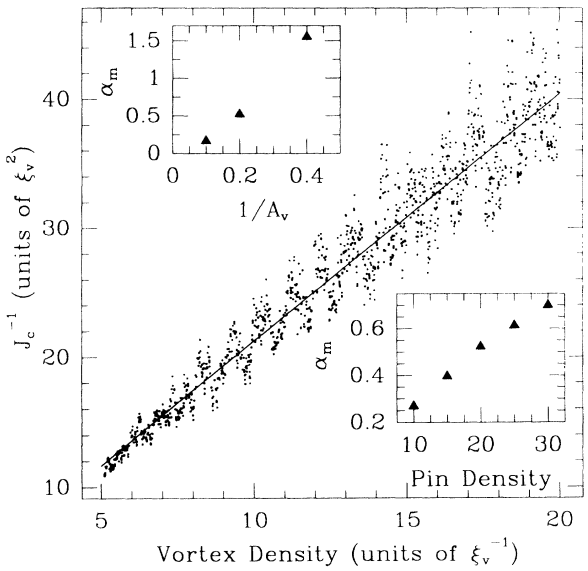

FIG. 3. $1/J_c$ for a sample with a pin density of 20 and $A_v = 5$. Solid line is a linear fit to the data. Insets show the dependence of the maximum pinning force α_m on $1/A_v$, corresponding to pinning strength and pin density. The values of α_m are obtained from linear fits like that shown in the main figure.

that this maximum force does not vary with field. The critical current at a given field is then found by equating the Lorentz force with α_m as in the following:

$$\alpha_m = J_c(H + B_0), \tag{3}$$

where α_m and B_0 are constants which depend on the microstructure of the material and H is the local field. This form implies that the inverse of J_c should depend linearly on field.

By performing linear fits to portions of profiles like those shown in Fig. 1 over a range of fields, we are able to extract the dependence of J_c on field in our samples. The inverse of J_c for one simulation is shown in Fig. 3. One can see that a linear dependence of this quantity on field describes the data very well. One can also observe from the plot an apparent oscillatory behavior superimposed on the linear trend in $1/J_c$. This is an artifact of the finite range of the vortex force, which results in a small discontinuity in the slope whenever the number of vortices within the force range of a given vortex increases by one. In a real sample, this change would happen gradually.

To further explore the relationship of our data to the Kim model of Ref. [7], we examined the dependence of the maximum pinning force α_m on pin density and the vortex-vortex force. Varying the latter quantity is equivalent to varying the pinning strength since it is the ratio of the pinning strength (defined as 1) to A_v which determines the behavior. The results are shown in the insets in Fig. 3. As expected, α_m increases monotonically with the number of pinning centers and with the pinning strength, $1/A_v$.

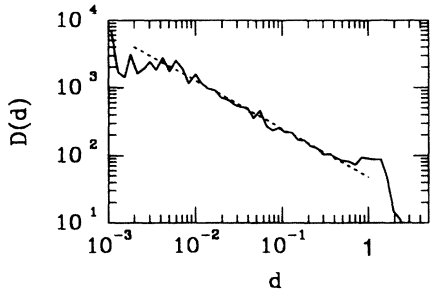

FIG. 4. Distribution of normalized average displacements for a simulation with pin density 20 and $A_v = 5$. The normalized average displacement, d, is plotted on the horizontal axis and $D(d)$, proportional to the number of events with a given d, is plotted on the vertical axis.

We also investigated the dynamics of the system after a single vortex has been added or subtracted. This was accomplished by evaluating the displacements of all the vortices in the system after each step. From this information, one can extract most dynamical quantities of interest. In particular, one can get an idea of the magnitude of the global motion of the system after a vortex addition or subtraction by calculating the average displacement of all of the vortices in the system at that step. Examination of this quantity is complicated by the fact that the properties of the system evolve as the vortex density changes. The individual displacements of vortices, and hence the global average, are generally smaller when the system is more highly filled since the motion of each vortex is constricted by the close proximity of its neighbors. The simplest solution of examining only a small portion of the simulation over which the properties of the system do not vary much places too severe a restriction on the statistics for this quantity. Our approach, then, consisted of normalizing the average displacement at each step according to that which would be expected for an unpinned periodic system with the same number of vortices. The average displacement for a vortex in an unpinned system can be shown to depend on total vortex number N as $L/4N$, where L is the length of the system.

By dividing the average displacement at each step by this normalizing function, we were able to eliminate any systematic trends in the data over the course of the simulation and thereby focus upon the statistical fluctations from step to step. The distibution of these normalized average displacements is shown in Fig. 4 for a simulation with a pin density of 20 per unit length, and $A_v = 5$. The ramp-up and ramp-down data were combined in this plot since, when examined alone, their distributions were comparable. We see power-law behavior over approximately 2.5 decades, with a slope of 0.71.

In addition, we examined the distribution of displacements of individual vortices in the system. Though this

quantity is more difficult to normalize, we see power-law behavior over approximately 2.5 decades here as well.

The theoretical treatment of the Bean model usually involves discussion of the Lorentz force on vortices. This force is proportional to the product of the local field and the current at that point. As emphasized by Brandt [6], the only way a macroscopic transport current can exist in a type-II superconductor is if it is accompanied by a gradient in the density of vortices or curvature of vortices. This is often a point of confusion in work on the subject of magnetic and transport properties of superconductors. In our simulation, no Lorentz force, *per se*, is applied to the vortices in the sample. They are simply driven into the sample by the repulsive forces between vortices. This repulsion, in conjunction with the interaction with attractive pinning centers, leads naturally to the development of a gradient in the vortex density, and vortices tend to move down this gradient. Now in a real sample, this gradient would necessarily, by Maxwell's equations, be accompanied by a current and one could describe the force on each vortex as being a Lorentz force which results from the interaction of current and magnetic field. Our work emphasizes the fundamental equivalence of these two outlooks; i.e., one can equally well describe the force on a vortex as being due to a Lorentz type process or as resulting from a greater repulsive force from the side of the vortex where there is a higher density of neighbors.

Another important result from our simulations is the natural development of a systematic decrease in J_c with increasing field. We stress again that the physical input into these simulations is very simple, consisting only of linear attractive and repulsive forces. That this is sufficient to derive a dependence of J_c on field that is consistent with experiment suggests that one need look no further to explain this behavior than that the increase in repulsive forces that accompanies an increase in field makes the pinning force, which does not vary with field, gradually less important.

From a dynamic point of view, there has been considerable interest and speculation about systems of the type under investigation here possibly exhibiting self-organized criticality (SOC) when driven to the threshold of instability. Many discussions of SOC in pinned flux lattices have relied on measurements or investigations of systems *relaxing away* from criticality [8,9], making them less than ideally suited for examining the SOC hypothesis. In our work, the system is truly driven to the threshold of instability and then allowed to organize itself into a critical state. In this manner, our simulations are analogous to slowly dropping sand on the top of a pile and observing the subsequent avalanches. It is generally believed that the strongest indicator of a system having an SOC character is for the distribution of dynamical events associated with that system to obey a power law. The average vortex displacements, shown in Fig. 4, are a measure of the overall "avalanche" activity in our systems at a given step. That this distribution follows a power law over more than 2 decades suggests that these systems may indeed be SOC in nature.

The authors would like to acknowledge useful discussions with S. Field and J. Witt. F.N. acknowledges partial support from a GE fellowship, a Rackham Grant, the NSF through Grant No. DMR-90-01502, and SUN Microsystems. O.P. is supported by a fellowship from Ministerio de Educación y Ciencia, Spain and by DOE Grant No. DE-FG-02-85ER5418.

* Present address: Instituto de Ciencia de Materiales (C.S.I.C.), Facultad de Ciencias C-III, Universidad Autónoma de Madrid, E-28049 Madrid, Spain.

† Author to whom correspondence should be addressed.

[1] C. P. Bean, Rev. Mod. Phys. **36**, 31 (1964).

[2] E. H. Brandt, J. Low Temp. Phys. **53**, 41 (1983); H. J. Jensen, A. Brass, A.-Ch. Shi, and A. J. Berlinsky, Phys. Rev. B **41**, 6394 (1990); H. J. Jensen, Phys. Rev. Lett. **64**, 3103 (1990).

[3] O. Pla and F. Nori, Phys. Rev. Lett. **67**, 919 (1991); (to be published).

[4] P. Bak, C. Tang, and K. Wiesenfeld, Phys. Rev. A **38**, 364 (1988).

[5] See, e.g., M. Tinkham, *Introduction to Superconductivity* (Krieger, Malabar, FL, 1985).

[6] E. H. Brandt, Physica (Amsterdam) **195C**, 1 (1992).

[7] Y. B. Kim, C. F. Hempstead, and A. R. Strnad, Rev. Mod. Phys. **36**, 43 (1964); Y. B. Kim, C. F. Hempstead, and A. R. Strnad, Phys. Rev. **129**, 528 (1963).

[8] V. M Vinokur, M. V. Fiegel'man, and V. B. Geshkenbein, Phys. Rev. Lett. **67**, 915 (1991).

[9] X. S. Ling, D. Shi, and J. I. Budnick, Physica (Amsterdam) **185-189C**, 2181 (1991).